Network single-walled carbon nanotube biosensors for fast and highly sensitive detection of proteins

2011 Nanotechnology 22 335502

(http://iopscience.iop.org/0957-4484/22/33/335502)

Nanotechnology **22** (2011) 335502 (7pp) doi:10.1088/0957-4484/22/33/335502

Network single-walled carbon nanotube biosensors for fast and highly sensitive detection of proteins

Pingán Hu[1], Jia Zhang[1], Zhenzhong Wen[1] and Can Zhang[2]

[1] Research Centre for Micro/Nanotechnology, Harbin Institute of Technology, No. 2 YiKuang Street, Harbin 150080, People's Republic of China
[2] Centre for Advanced Photonics and Electronics, University of Cambridge, Cambridge CB3 0FA, UK

E-mail: hupa@hit.edu.cn

Received 19 May 2011, in final form 11 July 2011
Published 26 July 2011
Online at stacks.iop.org/Nano/22/335502

Abstract
Detection of proteins is powerfully assayed in the diagnosis of diseases. A strategy for the development of an ultrahigh sensitivity biosensor based on a network single-walled carbon nanotube (SWNT) field-effect transistor (FET) has been demonstrated. Metallic SWNTs (m-SWNTs) in the network nanotube FET were selectively removed or cut via a carefully controlled procedure of electrical break-down (BD), and left non-conducting m-SWNTs which magnified the Schottky barrier (SB) area. This nanotube FET exhibited ultrahigh sensitivity and fast response to biomolecules. The lowest detection limit of 0.5 pM was achieved by exploiting streptavidin (SA) or a biotin/SA pair as the research model, and BD-treated nanotube biosensors had a 2×10^4-fold lower minimum detectable concentration than the device without BD treatment. The response time is in the range of 0.3–3 min.

S Online supplementary data available from stacks.iop.org/Nano/22/335502/mmedia

(Some figures in this article are in colour only in the electronic version)

1. Introduction

Incorporation of one-dimensional (1D) nanomaterials into the architecture of a field-effect transistor (FET) biosensor has been of great interest in the past decade [1, 2]. Owing to the reduced dimension, 1D nanomaterials including semiconducting nanowires and single-walled carbon nanotubes (SWNTs) have novel physical properties and high surface-to-area ratio, which make them useful for ultrahigh sensitivity FET biosensors [2, 3]. These 1D nanomaterial-based FET biosensors hold very promising applications for molecular diagnosis since they represent sensitive, label-free and easily miniaturized analytical ways, while traditional analytical techniques such as optical or spectroscopic methods require labeling agents or expensive and time-consuming procedures [4].

SWNTs are quantum wires with a diameter of ∼1 nm, comparable to the size of single biomolecules. SWNTs are entirely composed of a surface so that every carbon atom is in direct contact with the environment, allowing optimal interaction with biomolecules. Therefore, SWNTs are potentially used as a highly sensitive electrical transistor biosensor. Since the first demonstration of an SWNT-FET biosensor has been made by Start *et al* and Besteman *et al* [5, 6], an appreciable number of biosensing studies has been conducted by using SWNT transistors. SWNT-FET biosensors have been successfully demonstrated for the detection of various bio-targets such as DNA, protein, etc [7]. Initially, the SWNT biosensor was made from a single SWNT, which involved expensive and tedious electron beam (EB) lithography [5, 6]. Subsequently, a quantity of biosensors was performed on the network SWNT [8] since they are easier to fabricate than the one consisting of a single nanotube.

Sensitivity, which reflects minimum detectable concentration, is a key factor for a sensor. Much effort has been focused on sensitivity improvement of SWNT sensors. Ultrasensitive carbon nanotube (CNT)-based biosensors using antibody-binding fragments were reported [9]; the small molecule of

bisphenol A was detected with a picomolar limit by using an SWNT transistor functionalized with estrogen receptor-α [10]; femtomolar detection of 2,4-dichlorophenoxyacetic acid herbicides via competitive immunoassays using microfluidic-based CNT liquid-gated transistor has been discussed [11]. Recently, reported nanotube biosensors have shown reliable protein detection limits between 100 pM and 100 nM [8, 12, 13], while an approximate femtomoles of the protein detection limit has been achieved by Si nanowire devices [14]. The sensitivity is closely related to the sensing mechanism and configuration of the devices such as shape, thickness or surface modification of electrodes. In the case of nanowire device, the sensing protein is usually controlled by chemical gating [14]. SWNT devices are displayed as Schottky barrier (SB) transistors and their sensing mechanism seems more complex: four possible mechanisms were used to account for the variety in conductance of SWNT-FET biosensors. These proposed mechanisms are electrostatic gating, capacitance modulation, Schottky barrier (SB) effects and carrier mobility change [15–19]. Recently, Heller *et al* identified the sensing mechanisms of SWNT-FETs through convincing theoretical and experimental investigations [20]. Their results showed that sensing of SWNT-FETs was mainly operated by the SB effect as well as chemical gating; the SB effect would dominate especially when the isoelectric point (pI) of a protein was close to the pH of the reaction solution. This work inspires us to develop ultrahigh sensitivity biosensors using network SWNT-FET. The sensitivity can be enhanced through an increase in sensing area of the SB-operated network SWNT-FETs. Byon *et al* reported a percolated metal method for magnifying the sensing area of network SWNT-FET biosensors, whose detection limit was as low as 1 pM [21]. However, percolated metal in the network suppressed the FET effect of the device.

In this paper, we demonstrate a variety of methods to improve substantially the sensitivity of the SB effect operated network SWNT biosensor via an increase in sensing area. Conducting metallic SWNTs were cut or selectively removed by a controlled electric BD procedure; non-conducting metallic nanotubes were left for magnifying the sensing area. The lowest detection concentration of 0.5 pM was achieved from our SWNT biosensor.

2. Experimental section

Biotin-*N*-hydroxyl-succinimide ester (biotin) and streptavidin (SA, from Molecular Probes), bovine Immunoglobulin (IgG) (from Sigma-Aldrich), poly(ethyleneimine) (PEI, average molecular weight 25000, Aldrich) and poly(ethylene glycol) (PEG, average molecular weight 1000, Aldrich). High-resolution scanning electron microscopy (SEM, FEI Philips XL30 sFEG) was used to take images of network SWNT transistors. Raman spectra were measured at 632.8 nm excitation using Renishaw micro-Raman 1000 spectrometers. The electrical measurements were made using a probe station and a Keithley 4200 semiconductor parameter analyzer at ambient conditions. We grew the network SWNTs on SiO_2/Si by a reported chemical vapor deposition (CVD) method to fabricate such devices [22]. Subsequently, we prepared Ti/Au contacts on network SWNTs by a general photolithography process: the electrodes with 10/100 (Cr/Au) nm in thickness and a gap of $\sim$5 μm were made using a conventional UV lithography and lift-off technique. Conducting metallic tubes in the network were broken or removed by an electrical BD procedure with a high gate voltage (V_G = 15 V). The progress in the BD procedure was monitored by electrical measurements and Raman measurements. The nanotubes in the device were coated with a layer of PEI and PEG. These polymers were used for covalent attachment of biomolecules and prohibition of physical adsorption of proteins. To do so, the device was submerged in 5% water solution of PEI and PEG for 12–18 h, followed by rinsing in deionized water for 1 h. The polymer-coated devices were biotinylated by immersing them in a 10 mM water solution of biotin-*N*-hydroxysuccinimide ester at room temperature for 2 h. Subsequently, the biotinylated polymer-coated devices were used to detect SA by exposure of devices to the target solution with different concentrations at room temperature. To test the specificity of the biosensor, the device was exposed to 50 nM IgG in PBS buffer, which should not interact with the biotin layer. Also real-time monitoring of the electronic signal was carried out. The functionalized SWNT-FET was exposed to the SA with different concentrations. The sensing experiments were performed in a Teflon cell. The devices were installed into the cell and then filled with phosphate-buffered saline (PBS, 10 mM, pH 7.4) solution while 0.2 V of bias voltage (V_{ds}) was applied between the source and drain electrodes.The biological reaction was monitored by the measurement of an electrical response signal.

3. Result and discussion

Demonstration of a versatile method for an improved electrical break-down (BD) procedure to magnify the sensing area is a significant accomplishment in this work (as shown in figure 1). The SB area is to dominate sensing performance such as sensitivity and sensing speed in SB effect operated SWNT-FETs. The metallic nanotubes in the device are potentially used to magnify the SB area and thus improve the sensing area. As is well known, the present techniques always produce a mixture of metallic SWNTs (m-SWNTs) and semiconducting SWNTs (s-SWNTs). Our device consists of a mixture of m-SWNTs and s-SWNTs which could be proved by Raman characterization (shown in figure 2(d)). m-SWNTs in the network device were herein summarized into two sorts according to their configurations and performance (shown in figure 1): (1) refers to the conducting m-SWNTs which contact directly both electrodes; (2) refers to non-conducting m-SWNTs which just contact one electrode. We tried to cut or burn out the m-SWNTs selectively in air by using the electrical BD technique [22, 23]. In the BD, electric current flowed only in m-SWNTs, because s-SWNTs were depleted by the application of a high gate voltage (V_G = 15 V). Hence, only conducting m-SWNTs were burned out by the generated Joule heating [22]. We found that a higher V_{DS} or V_G (>20 V) easily burned out both the m-SWNTs and s-SWNTs. So we performed the cutting operation more

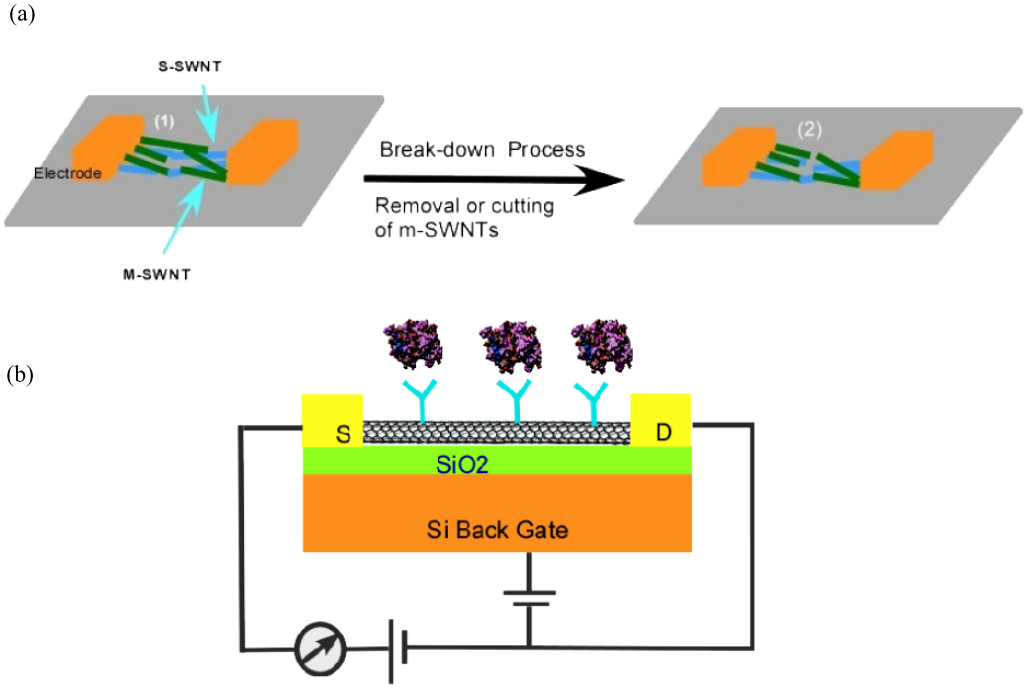

Figure 1. (a) Schematic drawing of the break-down process to remove or cut the conducting m-SWNTs, (1) represents the conducting m-SWNTs which contact two leads; (2) refers to the non-conducting m-SWNTs. (b) Schematic drawing for the carbon nanotube transistor biosensor with increased sensing area.

carefully: a relatively smaller V_{DS} (0–10 V) and V_G (15 V) was exploited. The operation of electrical BD is monitored by electrical measurements, scanning electron microscopy (SEM) and Raman characterization. Figure 2(a) showed a typical I_{DS}–V_G curve for the BD procedure which was completed within four scans. The drastic decrease in electric current for every scan indicated breaking or burning out of m-SWNTs. Figure 2(b) shows a typical transfer characteristic of I_{DS}–V_G curves before the BD and after the BD of the same device. The I_{DS}–V_G characteristics were largely improved after the BD. The on/off ratio which varied from less than 5 to 10^4 was achieved by controlling the V_{DS}, V_G and scanning rate. So the removal or cutting of conducting m-SWNTs can efficiently enhance the field effect of the device. The morphology of the device treated via BD was characterized by SEM (figure 2(c)). The SWNTs in the device were tangled together to form a network structure. The SWNT network with a gap of 3 μm and width of 1.5 μm contacted two electrodes. Due to the van der Waals interaction, the SWNTs in the device exist in the form of individual nanotubes or small bundles. Some nanotubes in images of figure 2(c) were broken in the section marked with arrows, and a zoomed picture clearly showed the structure of the broken section.

Raman spectroscopy is a powerful tool for non-destructive characterization of carbon nanotubes. The Raman measurement was performed with an excitation frequency of 633.2 nm on the same device before/after BD. The diameters of SWNTs are estimated to be typically 0.9–1.5 nm from the radial breathing modes (RBM). A detailed comparison with the plot of previous results allows us to conclude that the Raman peaks around 160–200 and 200–280 cm^{-1} are due to semiconducting and metallic SWNTs, respectively [24]. Raman spectra for the device treated via the BD process show weaker peaks of m-SWNTs around 200–280 cm^{-1} and stronger peaks around 160–200 cm^{-1}. This indicates that the metallic nanotubes were partly removed by the BD operation. Additionally, the distinct differences in shapes of the tangential G-band (approx. 1500–1620 cm^{-1}) offer a simple method to distinguish m- and s-SWNTs. Typically, the G-band for s-SWNTs has two distinct Lorentzian peaks (approx. 1590 and 1558 cm^{-1}) with relatively narrow linewidths. The peak at approx. 1590 cm^{-1} is associated with vibrations along the SWNT axis ($^+$G), while the peak at approx. 1558 cm^{-1} has been attributed to vibrations along the tangential direction ($^-$G). Although the $^+$G component of m-SWNTs has a Lorentzian lineshape that is almost as narrow as that for s-SWNTs, the $^-$G constituent is broad and best described by a Breit–Wigner–Fano (BWF) lineshape. So the comparable weaker and broader G-band after BD treatment provides additional evidence of m-SWNT elimination.

All the evidence of SEM, Raman and electrical measurements confirmed that the conducting m-SWNTs in the devices were removed or cut by the BD operation. The remaining non-conducting m-SWNTs were tangled together with s-SWNTs and acted in a role of an electrode, which increased the SB contact area. The biosensors made from this network SWNT FET had a larger sensing area and thus a higher sensitivity when the sensing was operated by the SD effect.

We investigated the improved sensitivity of devices with increased SB area by using non-specific binding and specific binding of SA (figure 3). The configuration of the biosensor is shown in figure 1(b). The silicon was used as the back

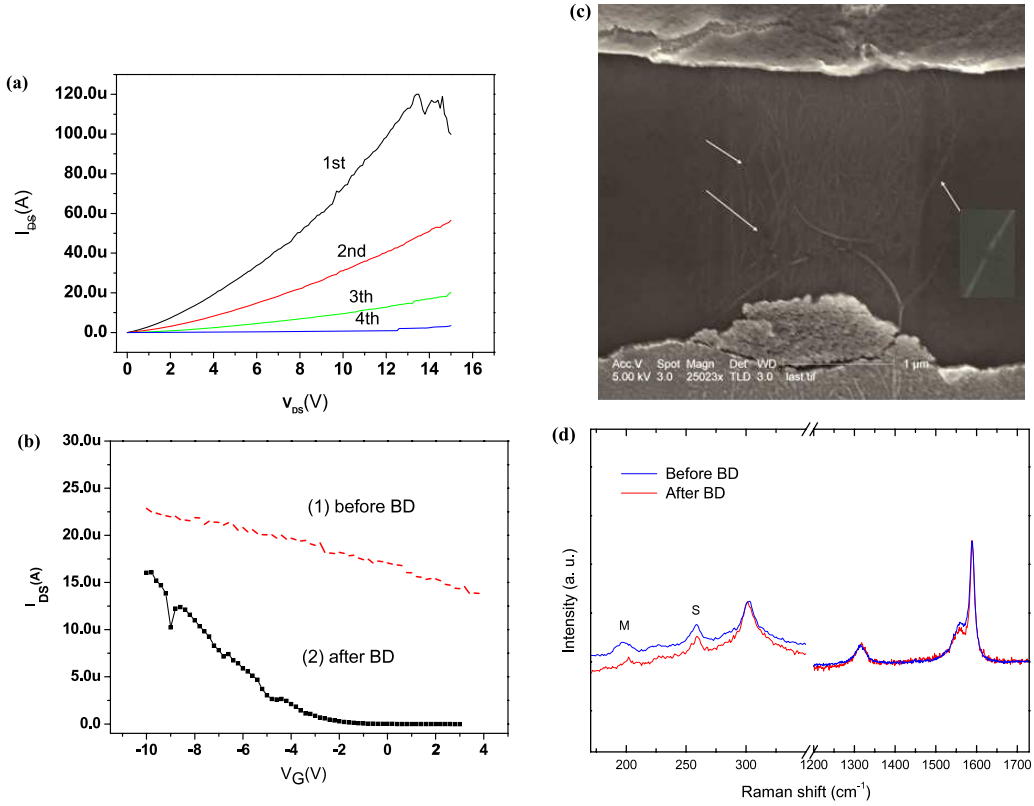

Figure 2. BD procedure was monitored by electrical measurement and SEM characterization: (a) curve of I_{DS}–V_{DS} ($V_G = 15$ V, scanning rate $= 0.25$ V S^{-1}); (b) curve of I_{DS}–V_G ($V_{DS} = 2$ V); (c) the morphology of a device which was treated via BD, the arrows marked the broken section and a zoomed image clearly shows the breaking of the nanotube by the electrical break-down technique. (d) Raman characterization of the same device before/after BD procedure.

gate. The sensing experiments were performed in a Teflon cell. When the devices started to show a steady current, proteins with specific concentrations were injected into the cell using a micro-syringe. The injection of protein was in the sequence from lower concentration to higher concentration so as to track the lowest detectable concentration for the as-fabricated biosensor. The real-time measurements were shown in figure 3. All of the examined devices have shown significant conductance drops (>1% conductance change) upon binding of proteins. As for non-specific binding of protein (shown in figure 3(a)), SWNT-FET with BD treatment was directly exposed to SA with progressively increased concentrations starting from 0.25 pM to 10 nm. This SWNT-FET started to respond to SA from 0.5 pM, which is determined as the detection limit for non-specific binding. After the addition of 1 nM SA into the Teflon cell, a small change in conductance could be observed. This net current value for 10 nM SA was much lower than the expected one. This could be caused by the full coverage of the SB contact with biomolecules after the addition of 1 nM SA. Thus the linear dynamic range for non-specific binding of SA was determined to be from 0.5 to 100 pM. The sensitivity is usually expressed as the output signal per concentration. The sensitivity of the non-binding of SA onto the bare SWNT-FET was estimated to be 30.5 nA pM^{-1} according to the results shown in figure S1 of the supporting data (available at stacks.iop.org/Nano/22/335502/mmedia).

To demonstrate sensing via a specific binding, the biotin/SA pair was exploited as a model in our study. Biotin is highly specific to SA [25]. SWNTs were coated with PEI and PEG polymers via hydrophobic interaction. The amino groups in PEI can be chemically bonded to the probe molecule of biotin. It has been reported that polymer coating can efficiently prohibit non-specific adsorption of biomolecules [13]. PEI and PEG are thus used to avoid the physical absorption of proteins on the nanotube surface. The selective and sensitive response to SA of the biotinylated SWNT-FET was shown in figure 3(b). The conductance also decreased with a progressively increased concentration. The biosensor showed no variation in current signal below 0.5 pM, so the minimum detectable concentration of specific binding was also 0.5 pM. The specific binding of proteins onto the SWNT-FET has already been performed in the literature: the reliable protein detection limits were given as between 100 pM and 100 nM [8, 10, 12, 13], which is higher than our result. As shown in figure 3(b), the conductance that was lower than the expected one could be observed after injection of 100 pM SA, and a much smaller change in current was obtained from the addition of 1 nM SA. This can be explained by the consuming of most of the attached biotin on nanotubes after the addition of 100 pM. The nonlinear detection range for specific binding here was from 0.5 to 1 nM. The sensitivity of the specific binding is about 27 nA pM^{-1} according to the results shown in figure S2 of the supporting data (available at stacks.iop.org/Nano/22/335502/mmedia).

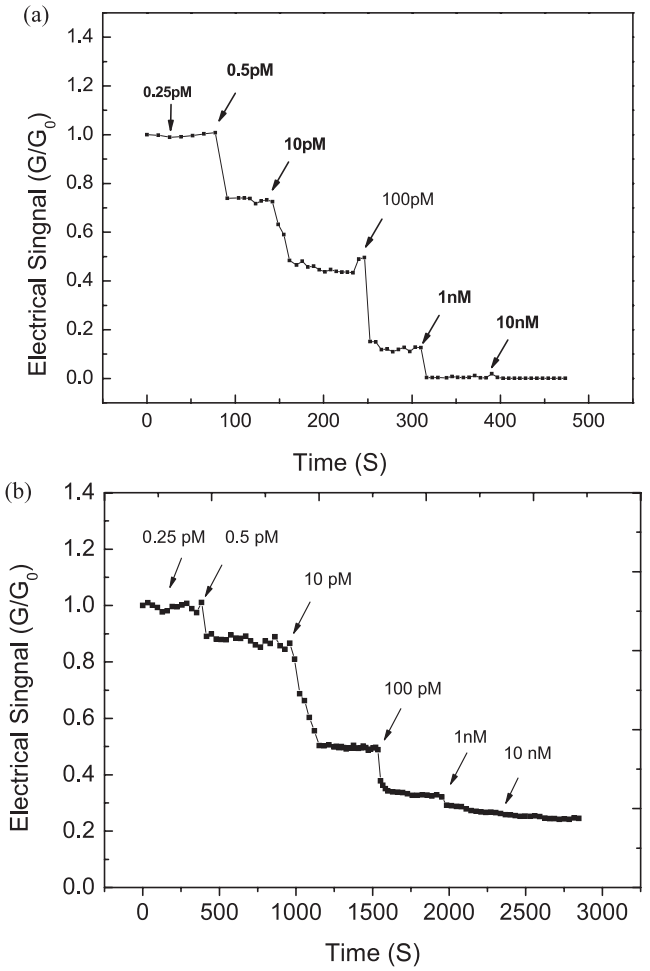

Figure 3. Time dependence of change in conductance normalized by initial conductance (G_0) ($V_{DS} = 0.2$ V) upon the binding of SA with different concentrations onto SWNT-FET with BD treatment: (a) non-specific binding on bare SWNT-FET and (b) specific binding on biotinylated SWNT-FET. The arrows indicate the point of sample addition.

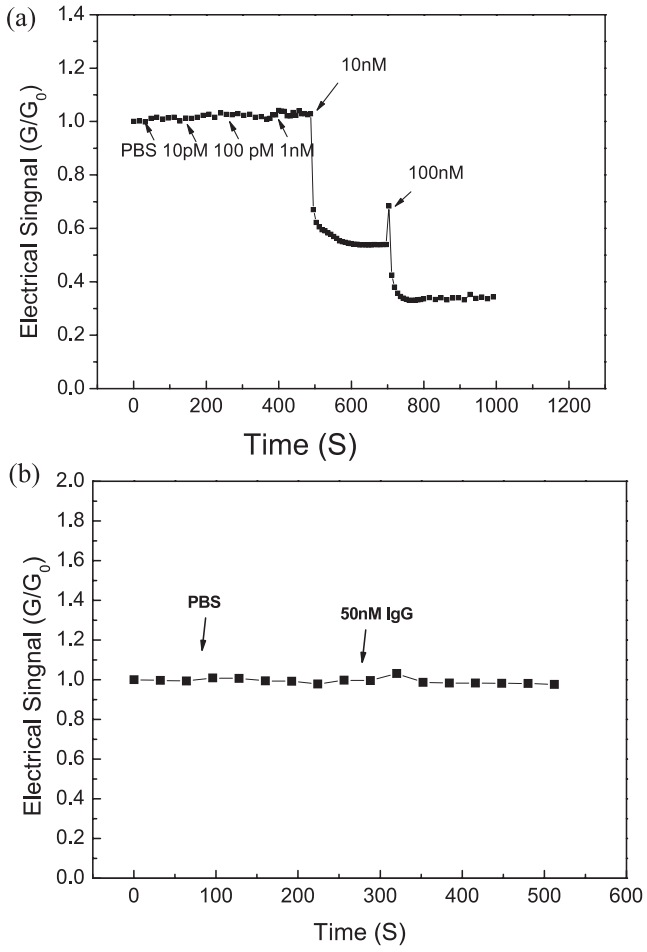

Figure 4. (a) Time dependence of change in conductance when normalized by using initial conductance (G_0) upon the introduction of target SA with different concentrations onto the biotinylated SWNT-FET without BD treatment (measured at $V_{DS} = 0.2$ V and $V_G = 0$). The arrows indicated the points of sample addition. (b) Time dependence of change in conductance normalized by initial conductance (G_0) upon the introduction of 50 nM IgG onto the biotinylated SWNT-FET with BD treatment (measured at $V_{DS} = 0.2$ V and $V_G = 0$): the arrows indicate the point of sample addition.

Our biosensor showed a fast response to the target protein: the conductance varied up to a steady level in a short time of 0.5–3 min after injecting SA with specific concentration (figure 3), which is much faster than current analytical methods such as spectroscopy. Comparing the results in figures 3(a) and (b), the non-specific binding exhibited a faster response. This could be attributed to different device configurations and working procedures of the two-type binding. In non-specific binding, the response time was mainly determined by the SA diffusion in solution; and bare SB contact was in direct interaction with protein, which may shorten the response period. While the response time in specific sensing was dependent on SA diffusion and biological recognition reaction between SA and biotin. In our experiments, non-specific binding of SA had a response period of 6–30 s and specific binding of SA to the biotin-modified SWNT device shows a slower response period of 18–90 s. We have tried 20 SWNT-FET biosensors treated via the BD procedure and obtained similar results, so our technique for the fabrication of a sensitive sensor was reproducible and reliable.

A comparable experiment was carried out on a device without the BD procedure treatment (shown in figure 4(a)). This device was also operated in the Teflon cell with a source–drain voltage of 0.2 V. The conductance as a function of injected SA concentration was shown in figure 4. The conductance of the device exhibited no change when injecting the samples with concentrations below 10 nM, while an obvious change in conductance started above 10 nM which is of course the detection limit. This limit was 2×10^4-fold higher than that of the nanotube device which was treated by BD. The results in figure 3S of the supporting data (available at stacks.iop.org/Nano/22/335502/mmedia) also showed that the biosensor started to respond to the SA with a concentration of 10 nM. In the range of 10–100 nM, the sensitivity was calculated to be 0.011 nA pM^{-1}, which was much lower than the biosensor treated by BD. Therefore, the BD procedure can enhance the sensitivity efficiently.

Further, we tested the specificity of our prepared SWNT biosensor with PEI and PEG coating by using IgG as the control protein. Injection of IgG (50 nm) did not change the conductance of the biosensor (shown in figure 4(b)), so the PEI and PEG coating could efficiently stop the non-specific binding (physical adsorption), and the conductance drops in figures 3(b) and 4(a) were attributed to the specific binding between the probe of biotin and target SA rather than any physical adsorption.

SWNT-FETs are operated as an unconventional Schottky barrier (SB) transistor. Protein adsorption on or very close to the SB contact is the key to conductance modulation and electrical sensing. Many reports have demonstrated that the SB contact is susceptible to modulation by adsorbed species [17]. The modulation of the metal work function can change the SB height of the metal–nanotube interface, leading to a change in the conductance of the device. The protein adsorption reduced the metal work function, and thus increased the Schottky barrier [13, 26]. So the conductance of our p-type SWNT-FET exhibited a decrease upon protein adsorption (proved by figures 3 and 4). Additionally, the variation of the electrode work function is closely related to the amount of adsorption species, so the conductance drops showed an obvious relationship to the protein concentration. That is why we got sensing signal curves with step-like drops of conductance upon the progressively increased concentration (shown in figures 3 and 4). Similar phenomena have been observed by other researchers [21]. Our BD-treated SWNT-FET exhibited a much lower detectable concentration compared to the device without BD treatment (shown by figures 3 and 4) thanks to the following possible reasons: firstly, the remaining metallic nanotubes increased the SB contact area and thus increased the sensing area, which was the principle for the enhanced response. Secondly, electrode geometry is crucial for device performance; rod-shaped electrodes can enhance the performance of the SB nanotube transistor [27], and the non-conducting metallic nanotubes worked as rod-like electrodes and improved the device performance.

The sensing mechanism of SWNT biosensors seems to be related to the configuration of the device such as surface modification, and the shape and structure of the electrodes. In this paper, SWNT biosensors with bare electrodes were controlled via an SB sensing mechanism, which is in accord with previous reports of SB-operated SWNT biosensors [17], while the SWNT-FET biosensor with gold electrodes coated with an octanethiol monolayer showed an increase in conductance upon exposure to the protein target and showed a chemical gating behavior in our previous work [28]. Dekker's group also demonstrated that this type of SWNT biosensor worked via a chemical gating effect [20].

4. Conclusions

In conclusion, we demonstrate the selective removal and cutting of m-SWNTs in the network nanotube FET via a careful control procedure of BD to construct an ultrahighly sensitive and fast biosensor. The conducting metallic nanotubes were selectively burned out or cut, and left non-conducting m-SWNTs acting in the role in magnifying the SB area. This nanotube FET exhibited ultrahigh sensitivity to proteins. The lowest detection limit of 0.5 pM was achieved, which is 2×10^4-fold lower than a nanotube FET sensor without BD treatment. The response time is 0.3–3 min for each concentration of the target. Our work on highly sensitive and fast SWNT devices is expected to accelerate progress towards the realization of nanoscale and label-free electronic biosensor systems.

Acknowledgments

This work is supported by the Scientific Research Foundation for the Returned Overseas Chinese Scholars, State Education Ministry and the Fundamental Research Funds for Central Universities and the Chinese Program for New Century Excellent Talents in University.

References

[1] Kauffman D R and Star A 2008 Carbon nanotube gas and vapor sensors *Angew. Chem. Int. Edn* **47** 6550–70
[2] Huang X J and Choi Y K 2007 Chemical sensor based on nanostructured materials *Sensors Actuators* B **122** 659
[3] Hu P, Zhang J, Li L, Wang Z L, O'Neil W and Estrela P 2010 Carbon nanostructure-based field-effect transistors for label-free chemical/biological sensor *Sensors* **10** 5133–59
[4] Lu J H, Strohsahl C M, Miller B L and Rothberg L J 2004 Reflective interferometric detection of label-free oligonucleotides *Anal. Chem.* **76** 4416–20
[5] Star A, Gabriel J P, Bradley K and Grner G 2003 Interaction of aromatic compounds with carbon nanotubes correlation to the hammett parameter of the substituent and measured carbon nanotube FET response *Nano Lett.* **3** 459
[6] Besteman K, Lee J, Wiertz F G M, Heering H A and Dekker C 2003 Enzyme-coated carbon nanotubes as single-molecule biosensors *Nano Lett.* **3** 727–30
[7] Star E Tu, Niemann J, Gabriel J C P, Joiner C S and Valcke C 2006 Label-free detection of DNA hybridization using carbon nanotube network field-effect transistors *Proc. Natl Acad. Sci.* **103** 921–6
[8] Kim J P, Lee B Y, Hong S and Sim S J 2008 Ultrasensitive carbon nanotube-based biosensors using antibody-binding fragments *Anal. Biochem.* **381** 193–8
[9] Nie T J, Wijaya P M, Wang Z, Goh W H, Palaniappan A, Mhaisalkar S G, Rodriguez I, Dunham S and Rogers J A 2009 Laminated.microfluidic-integrated carbon nanotube based biosensors *Appl. Phys. Lett.* **94** 013107
[10] Sánchez-Acevedo Z C, Riu J and Rius F X 2009 Fast picomolar selective detection of bisphenol A in water using a carbon nanotube field effect transistor functionalized with estrogen receptor-α *Biosensors. Bioelectron.* **24** 2842–6
[11] Wijaya P M, Nie T J, Gandhi S, Boro R, Palaniappan A, Hau G W, Rodriguez I, Suric R and Mhaisalkar S G 2010 Investigation of sensing mechanism and signal amplification in carbon nanotube based microfluidic liquid-gated transistors via pulsating gate bias *Lab on Chip.* **10** 634–8
[12] Kichambare A K D and Star A 2007 Carbon nanotube field-effect-transistor-based biosensors *Adv. Mater.* **19** 1439–51
[13] Chen R J, Bangsaruntip S, Drouvalakis K A, Kam N W S, Shim M, Li Y M, Kim W, Utz P J and Dai H J 2003 Noncovalent functionalization of nanotubes for highly

specific electronic biosensor *Proc. Natl Acad. Sci.* **100** 4984–9
[14] Zheng G, Patolsky F, Cui Y, Wang W U and Lieber C M 2005 Multiplexed electrical detection of cancer markers with nanowire sensor arrays *Nature Biotechnol.* **23** 1294
[15] Boussaad S, Tao N J, Zhang R, Hopson T and Nagahara L A 2003 *In situ* detection of cytochrome c adsorption with single walled carbon nanotube device *Chem. Commun.* **13** 1502
[16] Artyukhin A B, Stadermann M, Friddle R W, Stroeve P, Bakajin O and Noy A 2006 Controlled electrostatic gating of carbon nanotube FET devices *Nano Lett.* **6** 2080–5
[17] Gui E L *et al* 2007 DNA sensing by field-effect transistors based on networks of carbon nanotubes *J. Am. Chem. Soc.* **129** 14427–32
[18] Chen R J, Choi H C, Bangsarunti S, Yenilmez E, Tang X, Wang Q, Chang Y L and Dai H 2004 An investigation of the mechanisms of electronic sensing of protein adsorption on carbon nanotube devices *J. Am. Chem. Soc.* **126** 1563–8
[19] Tang X, Bansaruntip S, Nakayama N, Yenilmez E, Chang Y L and Wang Q 2006 Carbon nanotube DNA sensor and sensing mechanism *Nano Lett.* **6** 1632–6
[20] Heller I, Janssens A M, Mannik J, Minot E D, Lemay S G and Dekker C 2008 Identifying the mechanism of biosensing with carbon nanotube transistors *Nano Lett.* **8** 591–5
[21] Byon H R and Choi H C 2006 Network single-walled carbon nanotube-field effect transistors (SWNT-FETs) with increased schottky contact area for highly sensitive biosensor applications *J. Am. Chem. Soc.* **128** 2188–9
[22] Li Y, Kim W, Zhang Y, Rolandi M, Wang D and Dai H 2001 Growth of single-walled carbon nanotubes from discrete catalytic nanoparticles of various sizes *J. Phys. Chem.* B **105** 11424–31
[23] Collins P G, Arnold M S and Avouris P 2001 Engineering carbon nanotubes and nanotube circuits using electrical breakdown *Science* **92** 706–9
[24] Lazzeri M, Piscanec S, Mauri F, Ferrari A C and Robertson J 2005 Electron transport and hot phonons in carbon nanotubes *Phys. Rev. Lett.* **95** 236802
[25] Vajda S, Weng Z, Rosenfeld R and DeLisi C 1994 Effect of conformational flexibility and salvation on receptor-ligand binding free energies *Biochemistry* **33** 13977–88
[26] Cui X D, Freitag M, Martel R, Brus L and Avouris P 2003 Controlling energy-level alignments at carbon nanotube/Au contacts *Nano Lett.* **6** 783–7
[27] Appezeller J, Knoch J, Derycke V, Martel R, Wind S and Avouris P 2002 Field-modulated carrier transport in carbon nanotube transistors *Phys. Rev. Lett.* **12** 126801
[28] Hu P, Fasoli A, Park J, Choi Y, Estrela P, Maeng S L, Milne W I and Ferrari A C 2008 Self-assembled nanotube field-effect transistors for label-free protein biosensors *J. Appl. Phys.* **104** 074341